Improved Photovoltaic Properties of the Terpolymers Containing Diketopyrrolopyrrole and Isoindigo Side Chain

ARTICLE *in* POLYMER CHEMISTRY · FEBRUARY 2014

Impact Factor: 5.52 · DOI: 10.1039/C3PY01664A

7 AUTHORS, INCLUDING:

Zhencai Cao
Xiangtan University
18 PUBLICATIONS **157** CITATIONS
SEE PROFILE

Huajie Chen
Xiangtan University
36 PUBLICATIONS **715** CITATIONS
SEE PROFILE

Songting Tan
Xiangtan University
113 PUBLICATIONS **1,708** CITATIONS
SEE PROFILE

Polymer Chemistry

PAPER

Cite this: *Polym. Chem.*, 2014, **5**, 4054

Improved photovoltaic properties of terpolymers containing diketopyrrolopyrrole and an isoindigo side chain

Min Zhang,[a] Fen Wu,[a] Zhencai Cao,[a] Tianpei Shen,[a] Huajie Chen,[a] Xiangling Li[a] and Songting Tan*[ab]

Received 30th November 2013
Accepted 22nd February 2014

DOI: 10.1039/c3py01664a

www.rsc.org/polymers

A series of donor–acceptor (D–A) conjugated random terpolymers were synthesized by copolymerizing electron-rich alkylthienyl-substituted benzodithiophene (BDTT) and two electron-deficient units, a diketopyrrolopyrrole (DPP) moiety and isoindigo (TID) based side chain. The effects of the DPP and TID units on the thermal, photophysical and electrochemical properties of the polymers were investigated using thermogravimetric analysis, UV-vis-NIR absorption spectra, and cyclic voltammetry. Compared with the parent polymers (**P1** and **P2**), the optical properties of the random terpolymers (**P3–P6**) were controlled successfully by tuning the ratio of DPP and TID. The increase in TID content induced an increased absorption between 450 and 600 nm and a lower highest occupied molecular orbital (HOMO) energy level, while higher DPP content resulted in stronger absorption between 600 and 900 nm. Bulk heterojunction solar cells based on the as-synthesized polymers as electron donors and (6,6)-phenyl-C-butyric acid methyl ester (PCBM) as the acceptor were fabricated. The best power conversion efficiency (PCE) of 5.62% was obtained from **P5** (DPP : TID = 1 : 1) due to its high short-circuit current density (J_{sc} higher than 15 mA cm^{-2}), mainly arising from the broadened light absorption. The results have demonstrated that the random terpolymers, with complementary light-absorption, have a great potential for increasing the photocurrent and PCE in polymer solar cells.

Introduction

Polymer solar cells (PSCs) have been studied intensively as promising energy resources with the advantages of being flexible, light-weight, and having a low cost.[1–3] In the past few years, significant progress has been made in PSCs with power conversion efficiencies (PCEs) surpassing 10%.[4,5] Although progress has been impressive, the efficiencies of PSCs are still far from their inorganic counterparts.[5] One of the most effective approaches for enhancing PCEs is the development of novel conjugated polymers which exhibit broad light absorption with strong absorptivity, suitable energy level matching with the electron acceptor (fullerene derivatives), and appropriate morphology to promote charge separation and favorable transport of photogenerated charges.[5] As the limited absorption range results in lower short-circuit current density (J_{sc}, a key parameter for PCEs), a broad and intensive absorption is essential for a high PCE.[6]

One potential strategy towards broadening the absorption of the solar spectrum is to develop random terpolymers based on the copolymerization of one electron-rich unit and two different electron-deficient groups.[3,7,8] It's worth noting that a judicious selection of one electron-donating group with two different electron-deficient units is critical to achieve complementary and broad visible light absorption, thus maximizing photon harvesting.[9] As a class of brilliant red pigments, diketopyrrolopyrrole (DPP) has emerged as an interesting material in paints, plastic ink, electroluminescent devices, thin-film transistors, and PSC applications.[10,11] It possesses planar and well-conjugated skeletons that give rise to strong π–π interactions and result in absorptions in the near-infrared (NIR) region, especially at 600–900 nm.[12,13] Meanwhile, previous work has demonstrated that a new family of polymers with side chains has been successfully developed for PSCs.[14–18] Notably, the polymers with the side chain containing isoindigo (TID) exhibited excellent properties, including good film-forming and a deep-lying energy level of the highest occupied molecular orbital (HOMO). More importantly, there is strong absorption at 300–650 nm.[16] Based on the considerations above, the combination of DPP and TID electron-deficient units in a polymer backbone could be ideal for complementary and broad light absorption.[19]

Herein, we designed and synthesized a series of novel random terpolymers (Fig. 1) based on one electron-rich unit, alkylthienyl-substituted benzodithiophene (BDTT),[20] and two

[a]*College of Chemistry, Xiangtan University, Xiangtan 411105, P. R. China. E-mail: tanst2008@163.com*

[b]*Key Laboratory of Environmentally Friendly Chemistry and Applications of Ministry of Education, Xiangtan University, Xiangtan 411105, P. R. China*

electron-deficient units, DPP and TID, which have broad light absorption ranging from 300 to 900 nm. The much more broadened absorption of the as-synthesized polymers gave a great potential for improving the PSC performance and provided an ideal system for studying the effect of composition on the PSC performances. In terms of the ratio of DPP to TID, the PCEs of the polymers showed a non-linear compositional dependence from 0.67 to 5.62%. The best PCE value of 5.62% was obtained from the device of **P5** (DPP : TID = 1 : 1) blended with (6,6)-phenyl-C_{61}-butyric acid methyl ester ($PC_{61}BM$), showing a high J_{sc} value above 15 mA cm^{-2}. To understand the effects of DPP and TID on the non-linear compositional dependence of the PCE, the thermal, optical, electrical, and photovoltaic properties of these random terpolymers were systematically investigated.

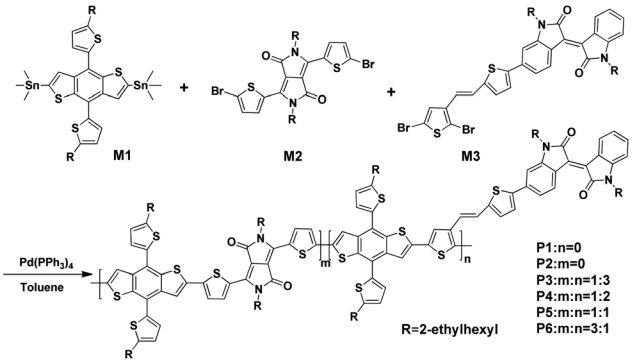

Scheme 1 Synthesis route of the polymers.

Experimental section

Materials and synthesis

The polymers were synthesized according to Scheme 1. The materials, (4,8-bis(5-(2-ethylhexyl))thiophen-2-yl)benzo[1,2-*b*:4,5-*b*'] dithiophene-2,6-diyl)bis(trimethylstannane) (BDTT, **M1**), 3,6-bis(5-bromothiophen-2-yl)-2,5-bis(2-ethylhexyl)pyrrolo [3,4-*c*]pyrrole-1,4 (2*H*,5*H*)-dione (DPP, **M2**), tetrakis-(triphenylphosphine)palladium(0) [$Pd(PPh_3)_4$] and molybdenum oxide (MoO_3) were purchased from Derthon Optoelectronic Materials Science and Technology Co., Ltd and Alfa Aesar. (*E*)-6-(5-((*E*)-2-(2,5-dibromothiophen-3-yl)vinyl)thiophen-2-yl)-1,1′-bis(2-ethylhexyl)-[3,3′-biindolinylidene]-2,2′-dione (**M3**) was synthesized according to the reported procedures.[16] Other reagents and solvents were purchased commercially with analytical-grade quality and used without further purification.

All the polymers were obtained *via* the Stille coupling reaction. Compounds **M1**, **M2**, and **M3** were dissolved in 20 mL of toluene in a flask protected by nitrogen. The solution was flushed with nitrogen for 30 min. $Pd(PPh_3)_4$ (5 mol%) was added under nitrogen and the mixture was flushed again with nitrogen for 30 min. Then, the oil bath was heated to 100 °C gradually, and the reaction mixture was stirred for 36 h at 100 °C under a nitrogen atmosphere. After cooling down to room temperature, the mixture was slowly poured into methanol (250 mL). The precipitate was collected by filtration and then purified by washing with methanol, hexane, and chloroform in a Soxhlet extractor for 24 h in sequence. The copolymers were obtained from the chloroform fraction by rotary evaporation.

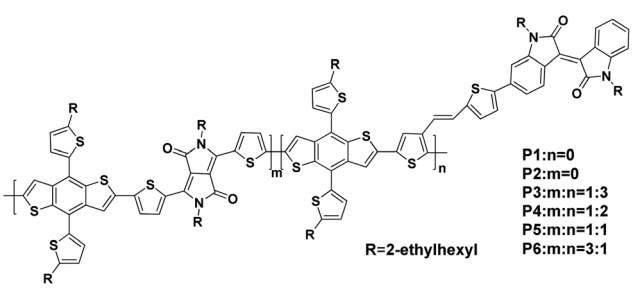

Fig. 1 Molecular structure of the polymers.

Polymerization for P1. A mixture of **M1** (120 mg, 0.13 mmol) and **M2** (91 mg, 0.13 mmol) in toluene was used to synthesize **P1** according to the procedure described above. The title polymer was obtained as a dark green solid, with a yield of 71%. ^{1}H NMR (400 MHz, $CDCl_3$, δ/ppm): 9.50–8.55 (br), 7.69–6.78 (br), 4.45–3.83 (br), 2.92–2.42 (br), 2.11–0.70 (br). Anal. calcd: C, 69.77; H, 7.32; N, 2.54; S, 17.46. Found: C, 68.34; H, 7.35; N, 2.47; S, 17.18%. M_n = 22.1 kg mol^{-1}, PDI = 4.37.

Polymerization for P2. A mixture of **M1** (120 mg, 0.13 mmol) and **M3** (111 mg, 0.13 mmol) in toluene was used to synthesize **P2** according to the procedure described above. The title polymer was obtained as an ash black solid, with a yield of 65%. ^{1}H NMR (400 MHz, $CDCl_3$, δ/ppm): 9.28–8.92 (br), 7.80–6.61 (br), 3.82–3.28 (br), 3.01–2.66 (br), 1.89–0.54 (br). Anal. calcd: C, 72.80; H, 7.07; N, 2.23; S, 15.34. Found: C, 70.63; H, 7.12; N, 2.19; S, 14.97%. M_n = 23.6 kg mol^{-1}, PDI = 1.92.

Polymerization for P3. A mixture of **M1** (150 mg, 0.16 mmol), **M2** (28 mg, 0.04 mmol), and **M3** (104 mg, 0.12 mmol) in toluene was used to synthesize **P3** according to the procedure described above. The title polymer was obtained as a puce solid, with a yield of 64%. ^{1}H NMR (400 MHz, $CDCl_3$, δ/ppm): 9.45–8.28 (br), 7.89–6.04 (br), 3.98–3.21 (br), 3.11–2.47 (br), 2.02–0.30 (br). Anal. calcd: C, 72.20; H, 7.01; N, 2.31; S, 15.84. Found: C, 70.96; H, 7.07; N, 2.28; S, 15.34%. M_n = 26.0 kg mol^{-1}, PDI = 2.23.

Polymerization for P4. A mixture of **M1** (150 mg, 0.16 mmol), **M2** (38 mg, 0.05 mmol), and **M3** (92 mg, 0.11 mmol) in toluene was used to synthesize **P4** according to the procedure described above. The title polymer was obtained as a puce solid, with a yield of 48%. ^{1}H NMR (400 MHz, $CDCl_3$, δ/ppm): 9.57–8.51 (br), 8.17–6.39 (br), 4.37–3.33 (br), 3.21–2.51 (br), 2.17–0.25 (br). Anal. calcd: C, 71.95; H, 7.04; N, 2.33; S, 16.01. Found: C, 70.65; H, 7.22; N, 2.31; S, 15.63%. M_n = 22.1 kg mol^{-1}, PDI = 2.85.

Polymerization for P5. A mixture of **M1** (150 mg, 0.16 mmol), **M2** (57 mg, 0.08 mmol), and **M3** (69 mg, 0.08 mmol) in toluene was used to synthesize **P5** according to the procedure described above. The title polymer was obtained as a dark green solid, with a yield of 78%. ^{1}H NMR (400 MHz, $CDCl_3$, δ/ppm): 9.52–8.30 (br), 7.86–6.42 (br), 4.27–3.40 (br), 3.30–2.67 (br), 2.08–0.34 (br). Anal. calcd: C, 71.44; H, 7.11; N, 2.38; S, 16.35.

Found: C, 69.97; H, 7.33; N, 2.36; S, 15.67%. $M_n = 22.4$ kg mol^{-1}, PDI = 1.92.

Polymerization for P6. A mixture of **M1** (150 mg, 0.16 mmol), **M2** (85 mg, 0.12 mmol), and **M3** (35 mg, 0.04 mmol) in toluene was used to synthesize **P6** according to the procedure described above. The title polymer was obtained as a dark green solid, with a yield of 60%. ^{1}H NMR (400 MHz, $CDCl_3$, δ/ppm): 9.39–8.39 (br), 7.66–6.66 (br), 4.55–3.78 (br), 3.49–2.36 (br), 2.15–0.31 (br). Anal. calcd: C, 70.70; H, 7.13; N, 2.46; S, 16.90. Found: C, 69.89; H, 7.34; N, 2.21; S, 16.13%. $M_n = 37.2$ kg mol^{-1}, PDI = 2.24.

Measurements and characterization

^{1}H NMR spectra were recorded on a Bruker AVANCE 400 spectrometer. The elemental analysis of all of the polymers was performed with an Elementar Vario EL III element analyzer. Ultraviolet-visible (UV-vis) spectra of the copolymers were obtained on a Perkin-Elmer Lamada 25 spectrometer. The average molecular weight and polydispersity index (PDI) of the polymers were determined using Waters 1515 gel permeation chromatography (GPC) analysis with THF as the eluent and polystyrene as the standard. Thermal analyses were performed on a Netzsch TG 209 analyzer under a N_2 atmosphere with a heating and cooling rate of 20 °C min^{-1}. Cyclic Voltammetry (CV) was conducted on an electrochemistry workstation (ZAHNER ZENNIUM) with the polymer film on a Pt plate as the working electrode, a Pt slice as the counter electrode, and a saturated calomel electrode (SCE) as the reference electrode in a 0.1 M tetra-*n*-butylammonium hexafluorophosphate (Bu_4NPF_6) acetonitrile solution. The scan rate was 50 mV s^{-1}. Atomic force microscopy (AFM) measurements were performed on a Digital Instruments Enviro Scope in a tapping mode.

Fabrication and characterization of photovoltaic devices

The photovoltaic cells were constructed with a traditional sandwich structure of ITO/MoO_3(10 nm)/polymer:PCBM/LiF(0.5 nm)/Al(100 nm).[21] Molybdenum oxide (MoO_3) was thermally evaporated on a cleaned indium tin oxide (ITO)–glass substrate giving a thickness of about 10 nm. The photosensitive active layer of the polymer and PCBM was prepared by spin-coating a chlorobenzene solution (10 mg mL^{-1}) on the surface of the ITO/MoO_3 electrode, and dried at 100 °C for 15 min in a nitrogen glove box. The cathode of the device, consisting of 0.5 nm of LiF and 100 nm of aluminum, was thermally deposited on the top of the copolymer blend film at 5×10^{-4} Pa. The thicknesses of the active layers were measured by an Ambios Technology XP-2 surface profilometer. The active area of the device was 3.8 mm^2. Current density–voltage (*J*–*V*) characteristics were measured using Keithley 2602 Source Measure Unit instrument controlled by a computer in the dark, under AM 1.5 illumination condition (100 mW cm^{-2}). The measurement of the monochromatic incident photon-to-current conversion efficiency (IPCE) was performed using a Zolix DCS300PA Data Acquisition System. All of these measurements were performed in an ambient atmosphere at room temperature.

Results and discussion

Scheme 1 outlines the general synthetic strategy that we used to obtain the random polymers. **M1** and **M2** were purchased from a commercial company. **M3** was synthesized according to the literature.[16] The polymerization reactions proceeded by the Stille coupling polymerization. The results and thermal properties of the polymers are summarized in Table 1. All of the polymers synthesized in this work have similar number-average molecular weights in the range of 20–40 kg mol^{-1} with high solubility in common organic solvents such as chloroform, tetrahydrofuran, and chlorobenzene.

Thermal properties

The thermal stability of the polymers was investigated by thermogravimetric analysis (TGA), as shown in Fig. 2. The TGA revealed that the decomposition temperatures (T_d) of the polymers (5% weight loss) were over 300 °C. Obviously, all of the polymers exhibited excellent thermal stability, which is important for their applications in PSCs and other optoelectronic devices.[22]

Optical properties

The optical properties of all of the polymers in the dilute chloroform solution and thin films are shown in Fig. 3 and summarized in Table 2. In the solution, the binary copolymer **P1** exhibits a major absorption band at 600–900 nm with a relatively high absorption coefficient of 6.6×10^4 (g mL^{-1})$^{-1}$ cm^{-1}. The other binary copolymer **P2** has a distinct absorption band in 300–600 nm with an absorption coefficient of 4.2×10^4 (g mL^{-1})$^{-1}$ cm^{-1}. As for the random terpolymers (**P3–P6**), the relative position and intensity of the absorption peaks were fine-tuned by changing the composition ratio of DPP and TID. By comparing their absorption spectra, a gradual blue-shift was observed when increasing the content of TID, which could be caused to a certain extent by the backbone twist between the main-chain and the side-chain of TID.[16,23] In addition, the increased amount of TID caused the appearance of a new absorption band around 450–600 nm, owing to the intramolecular charge transfer (ICT) band from BDTT to TID. Meanwhile, the absorption band around 600–900 nm originating from the ICT band from BDTT to DPP gradually decreased with the increasing content of TID. In the solid films, the absorption maxima of all the polymer films red-shifted in comparison with their solution absorptions, caused to a certain extent by aggregation of the polymer backbones.[24] Additionally, the optical band gaps (E_g^{opt}) of **P1–P6** were estimated to be 1.74, 1.51, 1.44, 1.46 1.26, and 1.37 eV, respectively, which were determined by the onset of their light absorptions.[25] Comparing to the parent polymers (**P1** and **P2**), the broad absorptions of the random terpolymers **P3–P6** were observed from 300 to 900 nm, indicating that the incorporation of two different electron-deficient units into a polymer backbone is an effective method to broaden the absorption band and control the optical band gap.

Table 1 Molecular weights and thermal properties of copolymers

Polymers	Yields (%)	M_n[a] (kg mol^{-1})	M_w[b] (kg mol^{-1})	PDI[c]	T_d[d] (°C)
P1	71	22.1	96.6	4.37	310
P2	65	23.6	45.4	1.92	374
P3 (DPP : TID = 1 : 3)	64	26.0	58.0	2.23	365
P4 (DPP : TID = 1 : 2)	48	22.1	63.1	2.85	367
P5 (DPP : TID = 1 : 1)	78	22.4	43.1	1.92	396
P6 (DPP : TID = 3 : 1)	60	37.2	83.3	2.24	379

[a] Number-average molecular weight. [b] Weight-average molecular weight. [c] M_w/M_n. [d] Decomposition temperature (5% weight loss) determined by thermal gravimetric analysis under nitrogen.

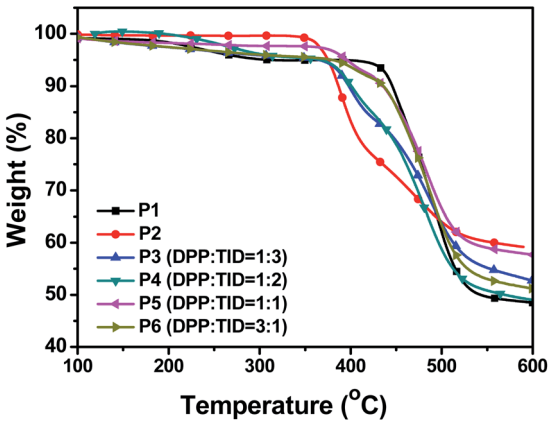

Fig. 2 TGA curves of the polymers with a scan rate of 20 °C min^{-1}.

Electrochemical properties

Cyclic voltammetry (CV) was employed to investigate the electrochemical properties of the polymers (Fig. 4). The corresponding data are summarized in Table 2. The redox potential of ferrocene (Fc) is 0.61 V *vs.* SCE. On the basis of 4.8 eV below vacuum for the energy level of Fc/Fc^{+25}, the HOMO and LUMO energy levels as well as the electrochemical energy gaps (E_g^{ec}) of the copolymers were calculated according to the following equations:

$$\mathrm{HOMO} = -\mathrm{e}(E_{ox} + 4.19)\ (\mathrm{eV})$$

$$\mathrm{LUMO} = -\mathrm{e}(E_{red} + 4.19)\ (\mathrm{eV})$$

$$E_g^{ec} = \mathrm{e}(E_{ox} - E_{red})\ (\mathrm{eV})$$

The onset potentials for oxidation (E_{ox}) were observed to be 0.99, 1.22, 1.39, 1.36, 1.47, and 1.04 V for **P1–P6**, respectively. The onset potentials for reduction (E_{red}) were −0.54, −0.49, −0.48, −0.54, −0.48, and −0.48 V for **P1–P6**, respectively. Accordingly, the HOMO energy levels of the binary polymers, **P1** and **P2**, were determined to be −5.18 and −5.41 eV, respectively. And the corresponding values of **P3–P6** were tuned by controlling the ratios of DPP to TID, with the data ranging from −5.23 to −5.66 eV. Meanwhile, similar calculations for the LUMO energy levels of all of the copolymers proceeded with the values ranging from −3.65 to −3.71 eV. Given the HOMO and LUMO energy levels, all of the polymers have enough driving force for efficient exciton dissociation with fullerene derivatives.[26] In Table 2, E_g^{ec} was slightly larger than E_g^{opt} due to the exciton binding energy of the organic conjugated materials.[10]

Film morphology

Film morphology is a key parameter to explain the difference in photovoltaic performance. Therefore, we employed AFM with a tapping-mode to investigate the morphology of the polymer:$PC_{61}BM$ (1 : 2, w/w) blend films. The height images and phase images of the polymers are shown in Fig. 5. It could be observed that the blend film of **P3** and **P6** exhibited relatively

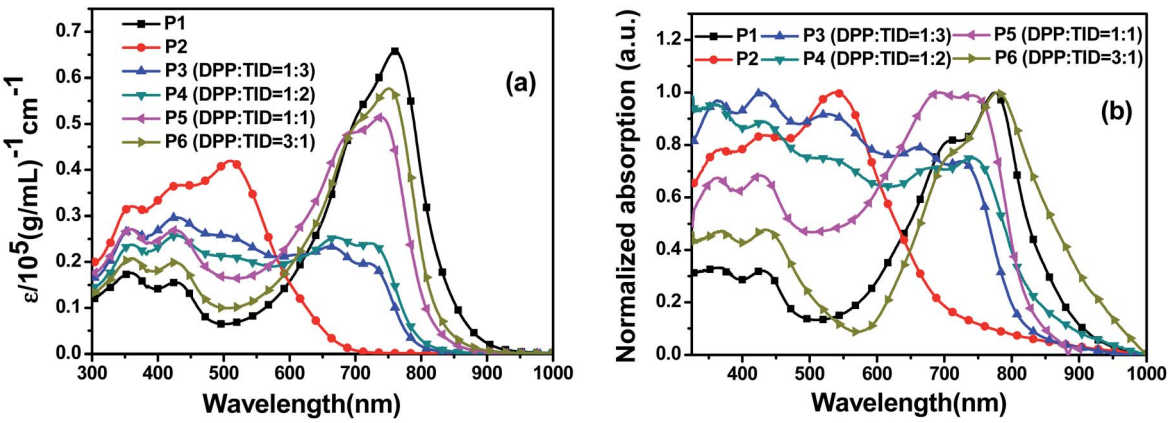

Fig. 3 UV-vis absorption spectra for polymers in chloroform solutions (a) and thin films (b).

Table 2 Optical and electrochemical properties of the polymers

Polymers	Solution $\lambda_{s,max}$ (nm)[a]	Film $\lambda_{f,max}$ (nm)[b]	E_g^{optc} (eV)	HOMO[d] (eV)	LUMO[e] (eV)	E_g^{ecf} (eV)
P1	760	777	1.37	−5.18	−3.65	1.53
P2	512	543	1.74	−5.41	−3.70	1.71
P3 (DPP : TID = 1 : 3)	665/723	663/730	1.51	−5.58	−3.71	1.87
P4 (DPP : TID = 1 : 2)	673/725	688/742	1.44	−5.55	−3.65	1.90
P5 (DPP : TID = 1 : 1)	700/737	691/738	1.46	−5.66	−3.71	1.95
P6 (DPP : TID = 3 : 1)	702/751	710/779	1.26	−5.23	−3.71	1.52

[a] Dilute chloroform solution. [b] Thin film spin-cast from the chloroform solution. [c] Optical band gap determined from the onset of absorption in the solid state. [d] HOMO energy level measured by photoelectron spectroscopy in air. [e] LUMO energy level measured by photoelectron spectroscopy in air. [f] $E_g^{ec} = -(E_{HOMO} - E_{LUMO})$ (eV).

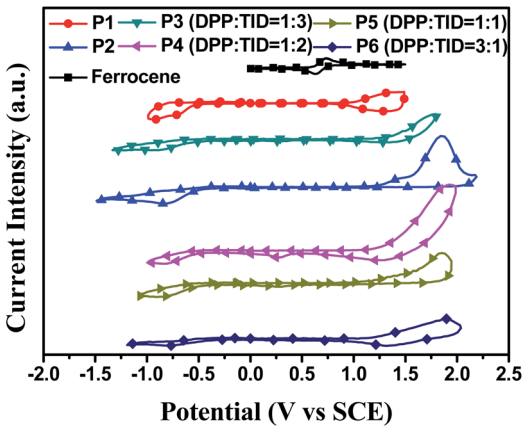

Fig. 4 Cyclic voltammograms of the polymer films on a platinum electrode in 0.1 mol L^{-1} Bu_4NPF_6 acetonitrile solution.

large phase separation (Fig. 5a and d), which went against the transfer of charge. However, the phase separation of **P4** and **P5** were improved and relatively homogeneous morphologies were achieved by tuning the ratio of DPP to TID. Compared with **P4**, an optimized nanoscale interpenetrating network of **P5** and $PC_{61}BM$ was obtained (Fig. 5c), which was beneficial for the charge transportation, thus leading to the highest J_{sc} as well as the highest device efficiency (Table 3 and Fig. 7).

Hole mobility

The charge carrier transport properties of conjugated polymers play a key role in the performance of PSCs. To understand the influence of charge carrier mobility of the polymers/$PC_{61}BM$ blend films on the photovoltaic properties, the hole mobilities of the target polymers were measured by a space charge limit current (SCLC) method.[27] Hole-only devices were fabricated with the configuration of ITO/PEDOT:PSS (25 nm)/polymer:$PC_{61}BM$/MoO_3(20 nm)/Al(100 nm). The hole mobility data of the copolymers are summarized in Table 3. The average hole mobilities ($\mu_{h,ave}$) of **P1**, **P2**, **P4**, **P5**, **P6** ranged from 1.0×10^{-5} to 2.9×10^{-5} cm^2 V^{-1} s^{-1}, which contributed to the enhanced J_{sc} of 6.58–13.71 mA cm^{-2} and the fill factor (FF) of 0.44–0.51 (Table 3).[28] As for **P3**, the value was 2.2×10^{-6} cm^2 V^{-1} s^{-1}, which was consistent with the inferior morphology measured by AFM in Fig. 5, leading to the relatively lower J_{sc} of 2.24 mA cm^{-2}.

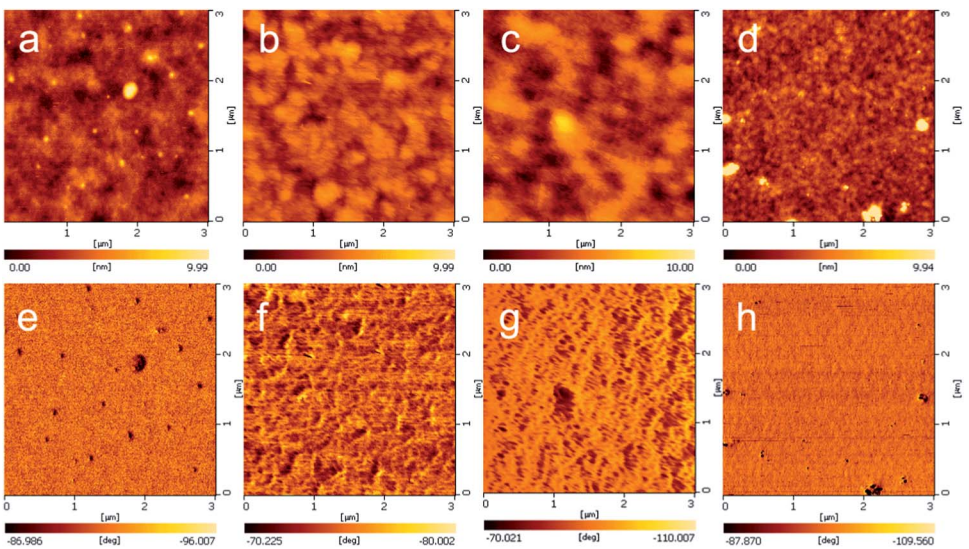

Fig. 5 Tapping-mode AFM height images (top) and phase images (bottom) for the blend films of terpolymers:$PC_{61}BM$ (1 : 2, w/w): (a and e) **P3**; (b and f) **P4**; (c and g) **P5**; (d and h) **P6**. All images size: 3 × 3 μm^2.

Table 3 Photovoltaic properties of the PSCs based on the as-synthesized polymers

Polymers	Solvent	J_{sc} (mA cm^{-2})	V_{oc} (V)	FF	PCE$_{max}$ (%)	$\mu_{h,ave}$ (cm^2 V^{-1} s^{-1})
P1[a]	CB	11.53	0.71	0.50	4.05	2.4×10^{-5}
P2[a]	CB	6.58	0.94	0.44	2.72	1.2×10^{-5}
P3 (DPP : TID = 1 : 3)[a]	CB	2.24	0.72	0.41	0.67	2.2×10^{-6}
P4 (DPP : TID = 1 : 2)[a]	CB	11.79	0.78	0.50	4.64	2.9×10^{-5}
P5 (DPP : TID = 1 : 1)[a]	CB	13.71	0.76	0.48	5. 02	1.3×10^{-5}
P5 (DPP : TID = 1 : 1)[a]	CB : CF = 7 : 3	15.13	0.76	0.49	5.62	—
P5 (DPP : TID = 1 : 1)[b]	CB	7.08	0.77	0.46	2.49	—
Blend (**P1** : **P2** = 1 : 1)[a]	CB	10.08	0.75	0.46	3.54	—
P6 (DPP : TID = 3 : 1)[a]	CB	10.08	0.74	0.51	3.75	1.0×10^{-5}

[a] The structure of fabricated devices: ITO/MoO_3(10 nm)/polymer:$PC_{61}BM$/LiF(0.5 nm)/Al(100 nm). [b] The structure of fabricated devices: ITO/MoO_3(10 nm)/polymer:$PC_{71}BM$/LiF(0.5 nm)/Al(100 nm).

Photovoltaic properties

To investigate whether the DPP unit and TID side group make a contribution to the power conversion efficiency in the PSCs, the bulk heterojunction (BHJ) PSCs for all of the polymers were fabricated with the ITO/MoO_3(10 nm)/polymer:$PC_{61}BM$/LiF(0.5 nm)/Al(100 nm) structure.[22,27] More than 10 devices were fabricated and their highest efficiencies and average values are provided in Table 3. The optimized weight ratios of polymers to $PC_{61}BM$ are 1 : 2, except **P1** (1 : 3). Fig. 6 shows the current density *versus* voltage (*J*–*V*) curves for the devices under AM 1.5 illumination at 100 mW cm^{-2}. The photovoltaic parameters, including the short-circuit current density (J_{sc}), the open-circuit voltage (V_{oc}), the fill factor (FF), and the power conversion efficiency (PCE), are summarized in Table 3.

From Table 3, the V_{oc} of **P1** is 0.71 V, which is comparable to the literature values.[13] **P2** exhibited the highest value of 0.94 V, probably caused by the larger backbone twists in the main-chain resulting from the TID side chain and the alkylthienyl substituents on benzodithiophene.[29] It is observed that the V_{oc} of the terpolymers ranges from 0.72 to 0.78 V. The non-linear trend is decided by a couple of other factors besides the HOMO levels of the polymers, such as the bulkiness of the side chains, interchain distances, and morphology of the active layers.[30,31]

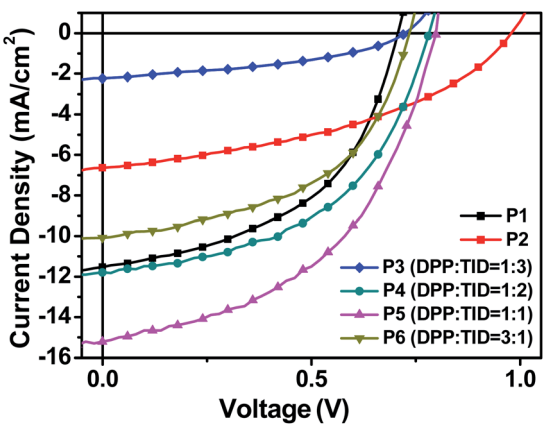

Fig. 6 *J*–*V* curves based on the polymers.

Furthermore, the PCEs of the random terpolymers showed a non-linear compositional dependence from 0.67 to 5.02% in the order: **P5** (5.02%) > **P4** (4.64%) > **P1** (4.05%) > **P6** (3.75%) > **P2** (2.72%) > **P3** (0.67%). In particular, **P5** exhibited the highest PCE value of 5.02% (J_{sc} = 13.71 mA cm^{-2}, V_{oc} = 0.76 V, FF = 0.48) among all of the polymers, which was attributed to the broad absorption and increased V_{oc} due to the deep-lying HOMO energy level. In contrast, the PCE decreased in the device of **P3** blended with $PC_{61}BM$ (0.67%), which mainly results from the significant decrease of the J_{sc}.

Based on the maximum efficiency measured from the device of **P5** blended with $PC_{61}BM$, several optimization processes were taken to improve the PCE. One process involved a mixture of chlorobenzene (CB) and chloroform (CF) as the processing solvent. The highest PCE of 5.62% (J_{sc} = 15.13 mA cm^{-2}, V_{oc} = 0.76 V, FF = 0.49) was achieved when the volume ratio of CB to CF was 7 : 3.[32] The other process used $PC_{71}BM$ as the electron acceptor. In spite of the better light absorption of $PC_{71}BM$, **P5** blended with $PC_{71}BM$ showed a lower PCE value of only 2.49%. In addition, physical blending of **P1** and **P2** with the weight ratio 1 : 1 was used as a reference with a lower PCE of 3.54% (J_{sc} = 10.08 mA cm^{-2}, V_{oc} = 0.75 V, FF = 0.46). The results demonstrated that developing random terpolymers based on the copolymerization is more effective than physical blending.

Meanwhile, PSCs based on the as-synthesized polymers blended with $PC_{61}BM$ were tested for their incident photon-to-current conversion efficiencies (IPCE). Typical curves are shown in Fig. 7. The IPCE spectra exhibited well-matched curves with their optical absorptions and a close correlation with their photocurrents in the *J*–*V* curves. The device based on **P1** exhibited two major responses, 300–500 nm and 500–900 nm, with a maximum IPCE of 45%. In comparison with the optical absorption profile of **P1**, it is clear that a large proportion of electron charge is generated from the absorption of PCBM.[5] As for **P2**, the device only exhibited a response from 300 nm to 650 nm, with a relatively low maximum IPCE of 50% at 447 nm. As shown in Fig. 7, the IPCE of **P3** was extremely low, which corresponds to the bad separation and transport of the photo-generated charges originating from the inferior morphology and the minimum hole mobility. Besides, the IPCEs of **P4**–**P6** in the range 300–900 nm were observed in all devices, suggesting

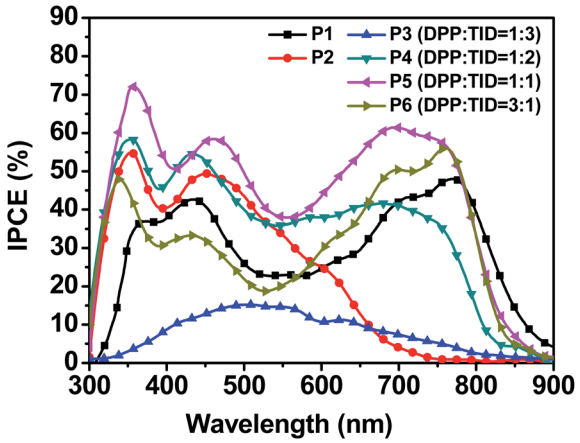

Fig. 7 IPCEs of the PSCs based on the polymers.

that the photon electron conversion processes were rather effective, which further demonstrated the better performance. Obviously, **P5** shows the highest IPCE among them, which is in line with the J_{sc}.

Conclusions

In summary, a series of novel random terpolymers with two electron-deficient DPP and TID building blocks were designed and synthesized to obtain polymers with complementary and broad light absorption from 300 to 900 nm for PSCs. UV-vis-NIR measurements revealed that the absorption spectra of the terpolymers were significantly tuned by varying the composition of DPP to TID in the polymers. The optimal ratio of 1 : 1 between DPP and TID in the random terpolymers increased the efficiency to 5.62% due to the improved light absorption and a high J_{sc} value of 15 mA cm^{-2}. The results demonstrate that synthesizing terpolymers composed of two different electron-deficient units with a complementary absorption range is an effective approach to extend the light absorption range of conjugated polymers for high performance PSCs.

Acknowledgements

This work was supported by the National Nature Science Foundation of China (no. 51173154), and the Nature Science Foundation of Hunan Province of China (12JJ7002, 13JJ2025).

References

1 B. Burkhart, P. P. Khlyabich and B. C. Thompson, *ACS Macro Lett.*, 2012, **1**, 660–666.
2 Y. Zou, A. Najari, P. Berrouard, S. Beaupré, B. Réda Aïch, Y. Tao and M. Leclerc, *J. Am. Chem. Soc.*, 2010, **132**, 5330–5331.
3 J. Jiang, H. Chen, H. Lin, C. Yu, S. Lan, C. Liu and K. Wei, *Polym. Chem.*, 2013, **4**, 5321–5328.
4 J. You, C. Chen, Z. Hong, K. Yoshimura, K. Ohya, R. Xu, S. Ye, J. Gao, G. Li and Y. Yang, *Adv. Mater.*, 2013, **25**, 3973–3978.
5 C. B. Nielsen, R. S. Ashraf, B. C. Schroeder, P. D'Angelo, S. E. Watkins, K. Song, T. D. Anthopoulos and I. McCulloch, *Chem. Commun.*, 2012, **48**, 5832–5834.
6 X. Guo, C. Cui, M. Zhang, L. Huo, Y. Huang, J. Hou and Y. Li, *Energy Environ. Sci.*, 2012, **5**, 7943–7949.
7 J. W. Jung, F. Liu, T. P. Russell and W. H. Jo, *Energy Environ. Sci.*, 2013, **6**, 3301–3307.
8 J. Song, C. Zhang, C. Li, W. Li, R. Qin, B. Li, Z. Liu and Z. Bo, *J. Polym. Sci., Part A: Polym. Chem.*, 2010, **48**, 2571–2578.
9 B. Burkhart, P. P. Khlyabich, T. Cakir Canak, T. W. LaJoie and B. C. Thompson, *Macromolecules*, 2011, **44**, 1242–1246.
10 T. E. Kang, H. Cho, H. J. Kim, W. Lee, H. Kang and B. J. Kim, *Macromolecules*, 2013, **46**, 6806–6813.
11 M. M. Wienk, M. Turbiez, J. Gilot and R. A. Janssen, *Adv. Mater.*, 2008, **20**, 2556–2560.
12 Y. Zou, D. Gendron, A. Najari, Y. Tao and M. Leclerc, *Macromolecules*, 2009, **42**, 2891–2894.
13 S. Zhang, L. Ye, Q. Wang, Z. Li, X. Guo, L. Huo, H. Fan and J. Hou, *J. Phys. Chem. C*, 2013, **117**, 9550–9557.
14 Z. Gu, P. Tang, B. Zhao, H. Luo, X. Guo, H. Chen, G. Yu, X. Liu, P. Shen and S. Tan, *Macromolecules*, 2012, **45**, 2359–2366.
15 Z. Gu, P. Shen, S. Tsang, Y. Tao, B. Zhao, P. Tang, Y. Nie, Y. Fang and S. Tan, *Chem. Commun.*, 2011, **47**, 9381–9383.
16 C. Wang, B. Zhao, Z. Cao, P. Shen, Z. Tan, X. Li and S. Tan, *Chem. Commun.*, 2013, **49**, 3857–3859.
17 X. Liu, Y. Huang, Z. Cao, C. Weng, H. Chen and S. Tan, *Polym. Chem.*, 2013, **4**, 4737–4745.
18 J. Hou, Z. Tan, Y. Yan, Y. He, C. Yang and Y. Li, *J. Am. Chem. Soc.*, 2006, **128**, 4911–4916.
19 S. Qu and H. Tian, *Chem. Commun.*, 2012, **48**, 3039–3051.
20 L. Huo, S. Zhang, X. Guo, F. Xu, Y. Li and J. Hou, *Angew. Chem., Int. Ed.*, 2011, **50**, 9697–9702.
21 F. Liu, S. Shao, X. Guo, Y. Zhao and Z. Xie, *Sol. Energy Mater. Sol. Cells*, 2010, **94**, 842–845.
22 L. Dou, J. Gao, E. Richard, J. You, C. Chen, K. C. Cha, Y. He, G. Li and Y. Yang, *J. Am. Chem. Soc.*, 2012, **134**, 10071–10079.
23 H. Kang, B. Zhao, Z. Cao, J. Zhong, H. Li, Y. Pei, P. Shen and S. Tan, *Eur. Polym. J.*, 2013, **49**, 2738–2747.
24 M. Zhang, Y. Sun, X. Guo, C. Cui, Y. He and Y. Li, *Macromolecules*, 2011, **44**, 7625–7631.
25 H. Li, H. Luo, Z. Cao, Z. Gu, P. Shen, B. Zhao, H. Chen, G. Yu and S. Tan, *J. Mater. Chem.*, 2012, **22**, 22913–22921.
26 T. E. Kang, H. Cho, C. Cho, K. Kim, H. Kang, M. Lee, S. Lee, B. Kim, C. Im and B. J. Kim, *ACS Appl. Mater. Interfaces*, 2013, **5**, 861–868.
27 Z. Gu, L. Deng, H. Luo, X. Guo, H. Li, Z. Cao, X. Liu, X. Li, H. Huang and Y. Tan, *J. Polym. Sci., Part A: Polym. Chem.*, 2012, **50**, 3848–3858.
28 M. Wang, X. Hu, L. Liu, C. Duan, P. Liu, L. Ying, F. Huang and Y. Cao, *Macromolecules*, 2013, **46**, 3950–3958.
29 Y. Li, *Acc. Chem. Res.*, 2012, **45**, 723–733.
30 H. Zhou, L. Yang and W. You, *Macromolecules*, 2012, **45**, 607–632.
31 W. Li, W. C. Roelofs, M. M. Wienk and R. A. Janssen, *J. Am. Chem. Soc.*, 2012, **134**, 13787–13795.
32 L. Ye, S. Zhang, W. Ma, B. Fan, X. Guo, Y. Huang, H. Ade and J. Hou, *Adv. Mater.*, 2012, **24**, 6335–6341.

